Permanent-Magnetically Amplified Robotic Gripper With Less Clamping Width Influence on Compensation Realized by a Stepless Width Adjustment Mechanism

Tori Shimizu, Kenjiro Tadakuma, Masahiro Watanabe, Kazuki Abe, Masashi Konyo, and Satoshi Tadokoro, *Member, IEEE*

***Abstract*—Machines such as robotic grippers use powerful actuators or gearboxes to exert large loads at the expense of energy consumption, volume, and mass. We propose a stepless force amplification mechanism that assists clamping by a pair of permanent magnets, in which the external control force required to adjust their distance, and thus the output force, is suppressed by compensation springs. For further sophistication, we invented a new width adjuster using a lever. By separating the actuation of fingers and compensated magnets temporarily, the adjuster eliminated the nonlinear influence of the object width on the clamping force. The prototype gripper for proof of concept revealed that the adjuster successfully linearized the width-force characteristic with an inclination of 0.15 N/mm, which is sufficiently insignificant compared to the major output force of approximately 50 N. The force amplification effect coexisted with this phenomenon, such that the clamping force was amplified to 137.5% while maintaining the energy consumption of a DC motor, and the force-energy efficiency was multiplied by 1.39. Thus, able to be driven by a weaker, smaller, and lighter actuator, the gripper contributes to extension of the operation time of robots with limited power.**

***Index Terms*—Actuation and joint mechanisms, force control, mechanism design.**

I. Introduction

MACHINES such as robotic grippers generally incorporate powerful actuators and massive gearboxes to exert a strong force or to bear a large load. However, this design method is inconvenient when applied to machines with strict volume and weight limitations. In other words, energy-efficient robotic components that can be driven by small and low-power actuators contribute to the extension of the mileage of the vehicles and the operation time of robots with limited power supply. Moreover, such efficient components reduce the cumulative electricity cost of a factory line in which robotic arms are repetitively used for long periods.

To achieve these desired features, spontaneous reduction mechanisms, passively driven by a main actuator to reduce the complexity of the control, have been proposed. These hardware approaches are especially advantageous in situations where signal transmissions of sensor and control may be interfered with, such as by radioactive rays. As exemplified in Fig. 2(a), load-sensitive grippers typically use mechanical joints such

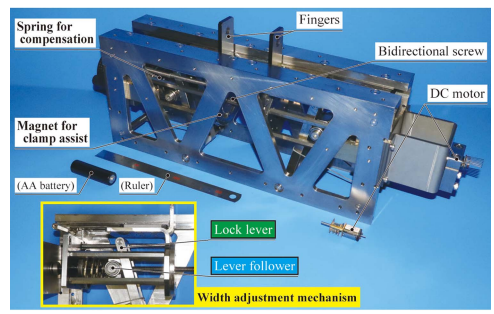

Fig. 1. Image of the proposed gripper using an internally balanced magnetic unit (IB magnet gripper) with a stepless width adjustment mechanism.

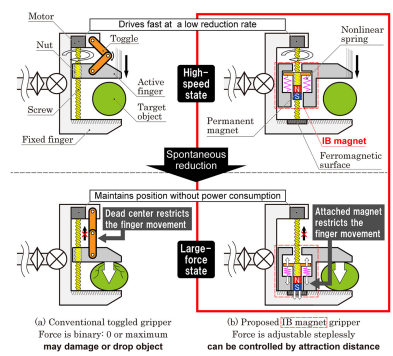

Fig. 2. Principle diagram of a conventional toggled gripper and the proposed IB magnet gripper.

Manuscript received 2 August 2022; accepted 17 November 2022. Date of publication 24 November 2022; date of current version 30 December 2022. This letter was recommended for publication by Associate Editor C.-H. Kuo and Editor C. Gosselin upon evaluation of the reviewers' comments. This work was supported by JSPS KAKENHI under Grant JP20J20184. *(Tori Shimizu and Kenjiro Tadakuma contributed equally to this work.) (Corresponding author: Kenjiro Tadakuma.)*

Tori Shimizu, Masashi Konyo, and Satoshi Tadokoro are with the Graduation School of Information Sciences, Tohoku University, Sendai, Japan (e-mail: shimizu.tori@rm.is.tohoku.ac.jp; konyo@rm.is.tohoku.ac.jp; tadokoro@rm.is.tohoku.ac.jp).

Kenjiro Tadakuma, Masahiro Watanabe, and Kazuki Abe are with Tough Cyberphysical AI Research center, Tohoku University, Sendai, Japan (e-mail: tadakuma@rm.is.tohoku.ac.jp; watanabe.masahiro@rm.is.tohoku.ac.jp; kazuki.abe.org@gmail.com).

This letter has supplementary downloadable material available at https://doi.org/10.1109/LRA.2022.3224664, provided by the authors.

Digital Object Identifier 10.1109/LRA.2022.3224664

This work is licensed under a Creative Commons Attribution 4.0 License. For more information, see https://creativecommons.org/licenses/by/4.0/

as toggles and clutches to switch from a high-speed state to a high-torque state [1], [2], [3]. However, they are not capable of adjusting the output force continuously because toggles tend to allow only a binary state of clamping, with either zero or maximum force. This is problematic when the robot needs to handle fragile objects without dropping and crushing them.

To solve these problems, we proposed a principle for the robotic gripper with force amplification [4], [5], in which a permanent magnet assists the clamping action through attraction, as shown in Fig. 2(b). Unlike binary toggles, magnets gradually and spontaneously increase the attractive force in proximity to the ferromagnetic surface, allowing the output clamping force to be adjusted in an analog (or, continuous) manner by shifting the implemented magnet in and out. Furthermore, the control force required to detach the magnet from the attraction target against its permanently exerted load is negated by the repulsive force of a spring so as to not affect the energy consumption of the actuator.

The prototype models in our previous research proved the basic principle of force amplification effect of the proposed gripper and realized a bi-parting symmetrical constitution for higher dexterity. However, as described in the next section, the compensation mechanism did not overcome the problem wherein the gripper has to adjust its clamping width arbitrarily, resulting in the unpredictability of the exerted clamping force according to the clamping width of the target object.

Therefore, in this study, we aim to develop a magnetically assisted gripper with an adjustment mechanism of the clamping width that allows the shifting of the force equilibrium point by latching the state of force transmission. By presenting a prototype of the gripper as a conceptual implementation instance, the study is conducted to provide a new point of view on the internal force compensation as an impact in the field of robotics, in expectation of leading future studies of its practical applications including, but not limited to, robotic manipulation.

This paper is organized as follows: In Section II, we briefly introduce the idea of the internal force compensation of a magnet, the core technology of this research, and its problems when applied to a gripper. Section III discusses the principle of the proposed magnetically assisted gripper mechanism with width adjustment ability. Section IV presents the experiments conducted to verify the effectiveness of the developed prototype model, and the results are discussed in Section V. Finally, Section VI presents the conclusions of this study.

II. Basic Principle

A. Magnetic Force Compensation

A compensation mechanism cancels out the operating force by applying an equal load in the opposite direction. For example, elevators, cranes, and robotic arms mount counterweights so that they can be actuated by a considerably smaller external force than their self-weight [6], [7].

To compensate for the magnetic attractive force, an "internally balanced magnetic unit (IB magnet)" was invented [8] and has been applied to robotic attraction devices [9], [10], [11], [12]. As illustrated in Fig. 3, the IB magnet comprises a magnet held by the control rod and a nonlinear spring connecting the control rod and the outer frame. The force-displacement characteristic of the spring $F_{\mathrm{r}}(x)$ is designed to be identical, but opposite in sign, to the characteristic of the magnet, $F_{\mathrm{m}}(x) = -F_{\mathrm{r}}(x)$, and it increases nonlinearly with its proximity x to the attracted

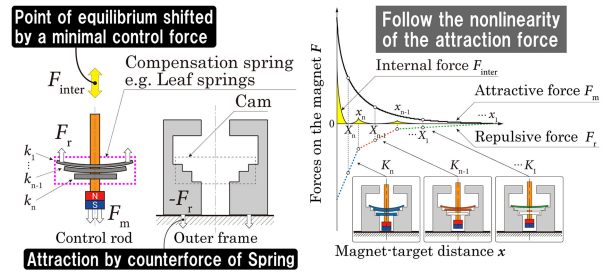

Fig. 3. Principle diagram of the IB magnet. The conventional nonlinear spring is composed of multiple linear springs that together work stepwise.

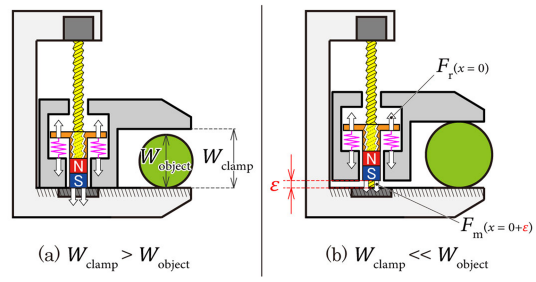

Fig. 4. Problems in the previous structure of the IB magnet gripper.

surface. Therefore, the more precise the spring is, the lesser the external force $F_{\mathrm{inter}} = F_{\mathrm{r}} + F_{\mathrm{m}}$ required to shift the control rod to attach and detach the magnet. Furthermore, the entire mechanism is attracted to the target object by the counterforce F_{r} exerted on the outer frame.

In the IB magnet gripper illustrated in Fig. 2, the frame of the IB magnet is extended as an active finger driven by an actuator and the ferromagnetic surface as a fixed finger. The actuator (here, a screw driven by a DC motor) shifts the active finger to the center of the gripper to fit the clamping width to the object width. Once the active finger meets the object, the control rod is pushed inward, increasing the clamping force exerted on the object between the outer frame and the fixed finger. When the sum of the thrust force of the actuator and the assisting magnetic attraction force exceeds the clamping force required to overcome the elastic force of the object, the magnet as well as the outer frame of the fixed finger reaches the attraction target.

To establish a bi-parting constitution of the fingers for higher versatility, the active fingers with IB magnets must be arranged plane-symmetrically with magnets facing opposite poles so that the internal forces on both fingers are compensated. The actuator must be replaced with a bi-parting feature such as a bidirectional screw.

B. Issues With the Previous Constitution

In our previous studies, there were some challenges in the constitutions wherein the IB magnet is simply inserted between the finger and the actuator; the finger is simply fixed on the outer frame of the IB magnet. First, as depicted in Fig. 4(a), the initial distance between the fingers defines the minimum clamping width of the gripper. If the object is even slightly thinner than the clamping width, the outer frames meet each other first before the fingers touch the object, resulting in a failure to clamp. Contrarily, if the object is extremely wider by ε than the clamping width, the initial distance of the magnet is insufficiently close to exert its attractive force, as described in

TABLE I
CATEGORIZATION OF CLUTCH MECHANISMS

	One direction only	Both positive & negative direction
Forward transmission only	Linear clutch (one-sided) [15] Force diode (one-sided) [16]	Linear clutch [17] Force diode [16] Torque diode [18]
Forward and inverse transmission	Sprag clutch Wire gripper [14]	(Rigid coupling)

Fig. 4(b). Therefore, the actuator has to push in the control rods of the IB magnets without sufficient assistance, resulting in an increase in energy consumption. If the elastic restoring force of the target object exceeds the thrust force of the actuator, the shift-in of the control rods may stop before attraction is attained.

These problems occur because the compensation of the IB magnet works under the major premise that the approaching displacement of the magnet is always equal to the compression distance of the spring. Although the magnet and spring have the origin of the stroke on the outer frame, the rod begins to be pushed in depending on the finger contact to the object rather than the outer frame contact to the attracted surface as the magnet and spring are fixed on the identical rod. Furthermore, interactive deformation of the spring and target object occurs closely linked to the progression of the actuator, making it difficult to predict the nonlinear clamping force characteristics according to the input force, actuation displacement, object width, and elasticity.

The previous gripper had a strict limitation on clampable object width and a complexity of nonlinear characteristics. As long as the width of the target object is known and fixed, e.g., the products in a factory line and the wheel to be braked [13], these inconveniences can be ignored. However, even then, their clamping width should be able to realign to handle a variety of products and brake pad wear. Therefore, a new mechanism has to be introduced so that the actuation of the compensation mechanism and the finger can be mechanically suspended when the fingers adjust the clamping width.

III. MECHANISM DESIGN

A. Categorization of Clutch Mechanisms

As the motivation to develop a gripper with a spontaneous reduction mechanism includes reducing the complexity of control, adding another actuator to adjust the clamping width must be avoided. In order for the proposed gripper to be versatile for any application by solving the abovementioned problems, adding a new passive mechanism is required that mechanically splits the IB magnet and the finger until the finger meets the object and then locks their relative position firmly when clamping is complete, so that the compensation of the magnet is independent of the absolute displacement of the finger. That is, the finger should be loosely connected to the IB magnet during its closing actuation, and the contact force of the target object must not be transmitted to the IB magnet. A linear one-way freewheel clutch, continuously activatable at any displacement and arbitrarily lockable by actuation, must be installed to realize such a separation of force transmission.

Table I categorizes the features of major existing clutches and similar mechanisms. Spring-tensioned rollers or sprags were used to transmit either rotational or translational movement by jamming between the input and output surfaces. In the table, "forward" is defined as force or displacement transmission from input to output, and "inverse" as from output to input, generally called a back drive. Furthermore, "positive direction" means one direction of the input rotation or translation (e.g., clockwise) and "negative" in the reverse direction (e.g., counterclockwise).

Observing the table, the mechanism that fulfills features required by the IB magnet gripper is totally unique in that it allows both forward and inverse transmission in the positive direction only when the outer frame detects its origin on the fixed finger. The wire gripper [14], a metal bracket to hang canvas art on a wire, has a feature to release the jamming state but is not applicable to the proposed gripper as it requires a feature to activate jamming.

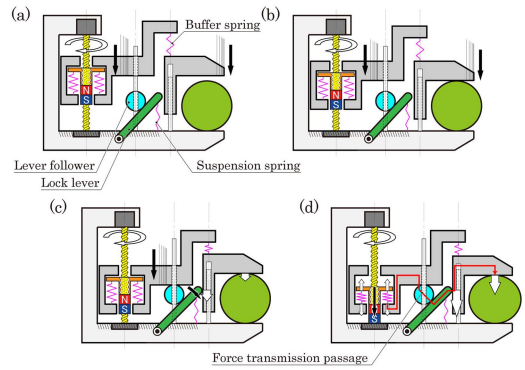

Fig. 5. Principle diagram of the IB magnet gripper with the width adjustment mechanism comprising a lock lever and a follower to push it down.

B. The Width Adjustment Mechanism Using Lock Lever

Fig. 5 depicts the IB magnet gripper with a newly devised width adjustment mechanism in which a lock lever and a circular lever follower are inserted between the outer frame of the IB magnet and the active finger. Assuming that they are rigid bodies, the lever and follower stay at a certain point, independent of the object width and pressing force. Therefore, the spring of the control rod can begin to get compressed at the identical displacement of the IB magnet in all instances. In this manner, this clutch enables the IB magnet to extract a pressing force from its fixed end of the spring, which was impossible as the spring had to be pinned in a designated position to sustain compensation.

The mechanism operates as follows. (a) Starting from the initial position, both the IB magnet and the active finger, loosely connected to the IB magnet via an adequately weak buffer spring, approach the target object. The lever is now disengaged by a separation spring and does not inhibit the actuation of the finger as the lever follower is still free. (b) Once the finger is in contact with the object, it stops further progress, resulting in the single actuation of the IB magnet. The buffer spring continues to get compressed to comply with the object width. (c) Next, when the outer frame of the IB magnet comes in contact with the lever follower, it starts to stretch the lever to lock the position of the finger relative to the outer frame of the IB magnet. The magnet approaches its attraction target with its designed actuation distance to be compensated. (d) Finally, the control rod of the IB magnet starts to move relative to the outer

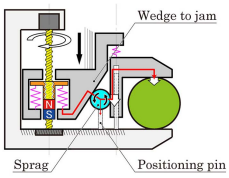

Fig. 6. Width adjustment mechanism composed of a sprag and wedge.

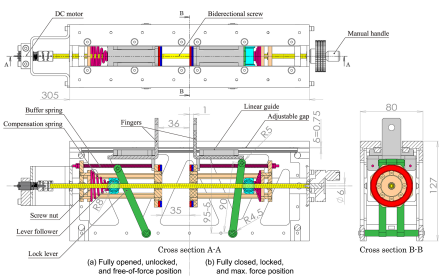

Fig. 7. Design of the prototype model of the IB magnet gripper. Some details are omitted, added, or exaggerated for better visibility. The colors of the components correspond to those of the elements in the diagram in Fig. 5.

TABLE II
SPECIFICATIONS OF THE PROPOSED IB MAGNET GRIPPER

Ring Magnet **NOR391**	*Outer Diameter*	54 [mm]	*Min. Clamping Width*	2 [mm]
	Inner Diameter	38 [mm]	*Max. Clamping Width*	72 [mm]
	Thickness	5 [mm]	*Stroke of the Control Rod*	35 [mm]
	Mass	40.8 [g]	*Total Mass*	5.7 [kg]
DC Motor **Pololu-3057**	*No-Load Performance*	35 [RPM], 80 [mA]		at 12 [V]
	Stall Extrapolation	176 [N·mm], 750 [mA]		
	Feed Speed	Approx. 1.0 [mm/s] with M6 screw		

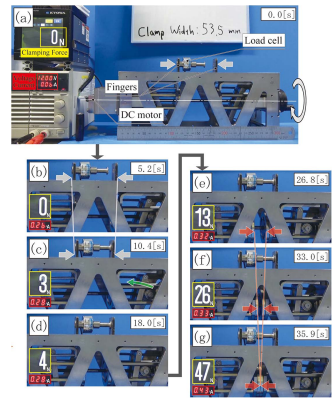

Fig. 8. Experimental system and the operation process of the prototype model of the IB magnet gripper. (a) The fingers were set 72 mm apart. (b) The screw began driving the control rods and fingers connected to them to the center. (c) The fingers stopped further actuation once they met the object. Instead, the buffer springs began to get compressed and the lock levers to lean against the fingers. (d) As the lock levers contacted the fingers, the control rods were ready to transmit force via the compensation springs. (e),(f) As the magnets approached each other, both the magnetic attractive force and the spring repulsive force increased, resulting in a stepless, gradual increase of the clamping force.

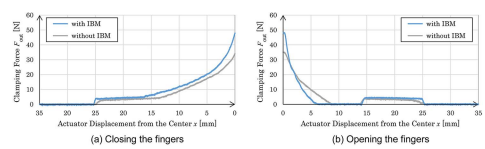

Fig. 9. A typical transition in the clamping force F_{out} of the IB magnet gripper with respect to the displacement x of the control rod of the IB magnet.

frame, increasing both the attractive force of the magnet and the repulsive force of the spring, resulting in the continuous increase of the force on the lever follower and thus the output clamping force.

Unlike existing clutches in Table I that use wedges and sprags to jam, herein, a pair of lever and follower were selected. As depicted in Fig. 6, the wedge was found to be unsuitable as its follower invaded the gap between the wedge and the active finger rolled along the wedge, feeding the finger in the reverse direction of the clamping motion. Furthermore, the sprag cannot be pinned at an arbitrary point as the pressing force from the IB magnet partially circumvents the finger via the positioning pin. This clutch can be used not only with the IB magnet, but also with other compensation mechanisms, such as those that balance a weight to a spring and output its repulsive force as a tension load.

IV. PROOF OF PRINCIPLE

A. Realization of the Prototype Model

Fig. 7 shows the dimensions of the prototype model of the proposed IB magnet in Fig. 1, whose specifications are listed in Table II. To prevent the increase in the mechanism volume, the axes of linear constraints, the bidirectional screw of the IB magnet, and the linear guide of the lever follower are arranged to coincide. Further miniaturization will be held in future to obtain a practical size and mass for integration to a robotic system. The distance between the contact surface of the finger and the axis of the lever is adjusted by inserting shims into the gap δ. Furthermore, the single conical coil spring with a varying diameter, and the pitch was customized to reproduce the nonlinearity of the magnetic attraction, unlike a bulky compensation spring in a conventional IB magnet comprising multiple linear springs that are activated stepwise to follow the nonlinearity approximately, as shown in Fig. 3.

B. Experiment 1: Basic Clamping Operation and Performance Evaluation

First, a basic operation experiment was conducted using the prototype of the proposed IB magnet gripper. Fig. 8 shows the system constituents and the experimental procedure, in which a load cell (Kyowa Electric, LUR-A-100NSA) was mounted on one of the active fingers to measure the compressive load to evaluate the effects of force amplification and internal force compensation. The DC motor was driven by a constant power supply of 12 V so that the current was proportional to the power consumption. The processes of clamping objects with widths $38.5 \leqq W_{\mathrm{obj}} \leqq 63.5$ mm, incremented by 5 mm by replacing stainless screws with corresponding lengths, were repeated five times for each contrasted configuration with and without magnetic attraction. Each IB magnet was initially arranged $x_{\max} = 35$ mm apart from the center, resulting in the initial distance between fingers $W_{\max} = 72$ mm.

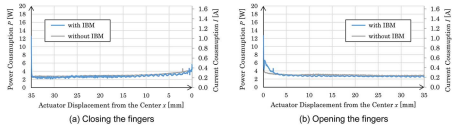

Fig. 10. A typical transition in the power consumption P of the IB magnet gripper with respect to the displacement x of the control rod of the IB magnet.

Figs. 9 and 10 display the typical transitions of the clamping force and power consumption measured with and without magnetic assistance when (a) closing and (b) opening the fingers to clamp the load cell with $W_{\text{obj}} = 53.5$ mm.

During closing, the clamping force first increased to an almost constant value, approximately $5\,\text{N}$, when the fingers contacted the load cell at the displacement $x = x_{\max} - (W_{\max} - W_{\text{obj}})/2 = 25.75$ mm. It kept slightly increasing in linearly, until the width adjustment by the buffer spring was completed. When the lever was first pushed onto the finger by the control rod via the compensation spring at $x = x_{\max} - X_{\text{f}}$ (discussed in Section V-A), the lever locked the position of the finger on the IB magnet. Then, as the spring further compressed, it transmitted the counter force to the lever follower, gradually increasing the clamping force. As the actuator can stop the position at an arbitrary displacement, the gripper can exert any desired value of the clamping force from zero to the maximum in an analog (or stepless) manner, as intended. With the aid of the magnets, the clamping force after the compensation spring was compressed became larger, while the power consumption remained almost unchanged from that of the constitution without magnets. This can be regarded as even slightly less due to the deviation of imperfect compensation, in which the internal force of the IB magnet that assists the actuation is oriented to the center of the gripper.

During opening, the clamping force is relieved gradually by releasing the compensation spring. After decreasing to zero, the clamping force is increased again as the lever releases the finger that clamps the object loosely with its buffer spring. The power consumption after inrush current at the beginning drops and then increases because the compensation is adjusted to be most precise at the origin where the attraction is originally the largest. The internal force after then inhibits actuation to some extent, contrary to the property observed during closing.

With the IB magnet, a $1\,\text{mm}$-periodic fluctuation of the power consumption was observed. It corresponds to the actuation by a lead screw with a pitch of $1\,\text{mm}$, whose thread stuck the edge of the dry bush of the magnet holder inclined due to gravity. To suppress this phenomenon, the bush shall be replaced with a longer one or one with a stricter fitting.

Fig. 11 illustrates the characteristic of the maximum clamping force characteristic with respect to the object width with and without magnetic assistance. F_{ave} is defined as the average value of the force measured for 1 s in a static state after the closing and the current cut off, while $F_{\max}$ is the maximum value recorded during the closing operation.

Both F_{ave} and $F_{\max}$ show similar increasing transitions for each constitution, while the former exceeds the latter by less than 1.9% for any condition (Let F_{ave} represent the maximum clamping force hereafter). The existence of the magnet increased F_{ave} to 137.5% in average, verifying the effectiveness of the magnetic assistance in generating clamping force by its attraction movement.

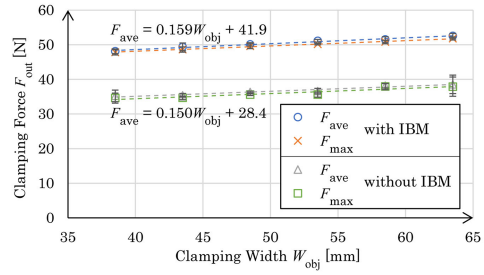

Fig. 11. Five-time average maximum clamping force $\max(F_{\text{out}})$ exerted by the IB magnet gripper with respect to the clamping width W_{obj}.

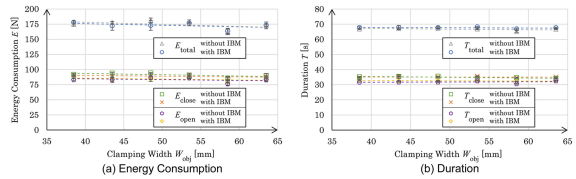

Fig. 12. Five-time average energy consumption E and duration T recorded on the IB magnet gripper with respect to the clamping width W_{obj}.

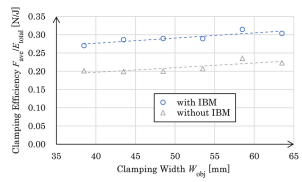

Fig. 13. Clamping efficiency of the IB magnet gripper defined as the average maximum clamping force F_{ave} divided by the average energy consumption E_{total} with respect to the clamping width W_{obj}.

Notably, F_{ave} and $F_{\max}$ show linear characteristics with inclinations around $0.15\,\text{N/mm}$, corresponding to the nominal theoretical range of 0.131–$0.160\,\text{N/mm}$ of the spring constant of the buffer spring for width adjustment. By selecting an even weaker buffer spring, the dependence on the clamping width can be reduced further. This property of consistency is important for a gripper to be easily predictable and thus controllable. This was not accomplished in our previous structure with a nonlinearly convex width-force characteristic seesawing from 60 to 110 N in a tolerable clamping width range of only $8\,\text{mm}$.

Fig. 12 shows the (a) energy consumption as an integration of the power consumption and (b) duration, measured separately during closing, opening, and the entire process. As visually observed in Fig. 10, the compensation mechanism slightly decreased E_{close} and increased E_{open} so that their sum E_{total} was barely affected: it just decreased by 0.8%.

Contrary to the clamping force, both energy and duration showed unsteady but similar transitions, fluctuating with deviation less than 4.5% for energy and 1.7% for duration. This observation implies that these characteristics are affected by other environmental factors such as lubrication and motor heating rather than the clamping width. The reason why these characteristics resemble each other is simple: the longer the duration, the more the power consumption.

Fig. 13 depicts the performance efficiency of the gripper, an index defined by the maximum clamping force F_{ave} divided by the total energy consumption E_{total}. As the F_{ave} was linear to

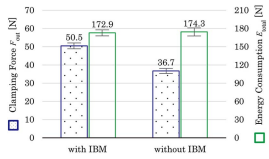

Fig. 14. Comparison of the results of measuring the maximum clamping force F_{ave} and energy consumption E_{total} under constitutions with and without IB magnet.

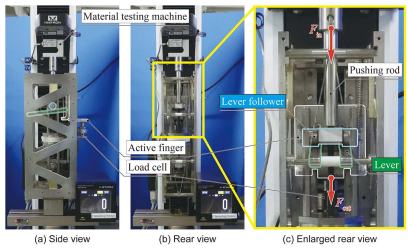

Fig. 15. Experimental system of the IB magnet gripper for measuring the transmission efficiency of its lever-follower clutch system.

W_{obj} and the E_{total} was independent of W_{obj}, the graphs of their quotient also show linear characteristics. For a better intuitive understanding, average results of F_{ave} and E_{total} in the range of W_{obj} are compared in Fig. 14. While the clamping force was amplified by the magnetic attraction, an additional external force required by the control rod to the actuator to push in and pull out the magnet against the attractive force was cancelled out by the repulsive force of the compensation spring, resulting in multiplication of the force-energy efficiency by 1.39 in the mean.

In these ways, the experiment successfully validated the principle of the proposed gripper by demonstrating characteristic-steady, force-amplified, and energy-efficient clamping ability against objects of various widths.

C. Experiment 2: Transmission Efficiency of the Lever-Follower System

The output clamping force was measured in relation to the input pressing force applied to the lever follower to derive the transmission efficiency of the width adjustment mechanism. The system constituents are shown in Fig. 15, wherein the gripper is installed vertically in the material testing machine (Instron, 3343). The finger below is fixed at the center of the system, and the finger above is free of mechanical restraints except the linear guides. The moving part of the material testing machine is equipped with a force transducer (Instron, 2516-104) with the capacity of 500 N to regulate the constant input force $25 \leqq F_{\text{in}} \leqq 300$ N incremented by 25 N, and a cylindrical rod to push down the lever follower. The gripper clamped the load cell with $W_{\text{obj}} = 38.5$, 43.5, and 48.5 mm five times for each configuration. Furthermore, for evaluating the effect of friction on the transmission, a friction-improved version of the lever-follower system was inspected. As contrasted in Fig. 16, its contact surface of the finger to the lever was matt-finished by rough electrical discharge machining, and the tip shaft of the lever that contacts the finger was substituted with one with straight knurling.

Fig. 17 compares the results of the measurements of the input-output force characteristics and the average transmission

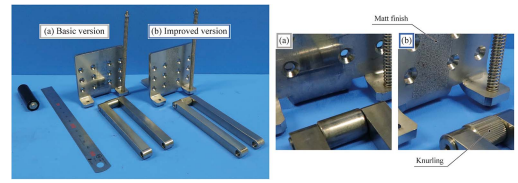

Fig. 16. Appearance of the (a) basic version and (b) friction-improved version of the lever and the contact surface of the finger.

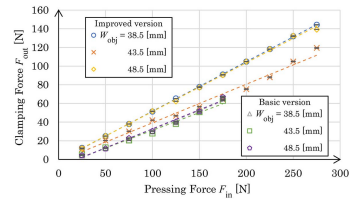

Fig. 17. Five-time average output clamping force F_{out} exerted by the lever-follower transmission mechanism with respect to the input pressing force F_{in}.

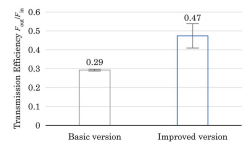

Fig. 18. Comparison of the transmission efficiency defined as the average output clamping force F_{out} divided by the average input pressing force F_{in}.

efficiencies are listed in Fig. 18. Due to the deformation, the lever broke through its leaning position against the contact surface of the finger with an input force larger than 175 N for the basic version, resulting in "unlocking" of the finger and thus no further records. This implies that the rigidity of the mechanism, especially the lever, should be increased to avoid this phenomenon without improving friction.

As the graphs show constant inclinations, the average transmission efficiency was stable around 0.29 independent of the clamping width for the basic version and increased to 0.47 for the friction-improved version, indicating that enhanced friction would multiply the clamping force and thus the force-energy efficiency of the gripper by 1.62. However, the result of the measurement under the condition $W_{\text{obj}} = 43.5$ mm for the improved version was notably inconsistent with other results. The cause of this outlier would be the difference in the engagement position of the knurling of the lever tip in contact with the finger. By replacing the lever tip with a continuously rough surface similar to the finger, the fluctuation could be avoided and the transmission efficiency could be further increased.

V. Discussion

A. Transmission Efficiency

Referring to the dimensions in Fig. 7, the transmission efficiency of the lever-follower system in the width adjustment mechanism can be estimated as follows:

Fig. 19 illustrates how a follower is in contact and pressed against the lever with F_{in} at point $\mathbf{P}$ by the pressure angle α. The force applied by the follower is partitioned into those perpendicular and parallel to the surface of the lever, and then into directions perpendicular and parallel to the actual moment arm

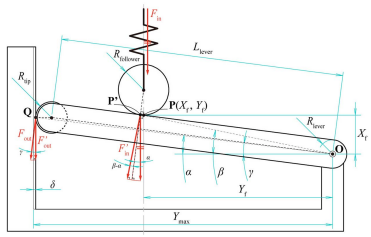

Fig. 19. Definition of the coordinate systems, variables, and forces of the lever-follower transmission.

OP with elevation β, resulting in the effective force component F'_{in} expressed as follows:

$$F'_{\text{in}} = F_{\text{in}} \cos\alpha \cos(\beta - \alpha) \tag{1}$$

Here, the elevation angle α of the lever tangent to the finger at **Q** equals the pressure angle of the lever follower, which is expressed by design constants as follows:

$$\alpha = \cos^{-1} \frac{Y_{\text{max}} - (R_{\text{tip}} + \delta)}{L_{\text{lever}}} = 7.4^\circ \tag{2}$$

The torque T_{out} applied to the finger by the tip of the lever is that generated by the follower $T_{\text{in}} = F'_{\text{in}} L_{\text{OP}'}$. $L_{\text{OP}'}$ is the length of the actual moment arm of the actual contact point of the follower $\mathbf{P}'(X'_{\text{f}}, Y'_{\text{f}})$ to the lever axis **O**, expressed by the coordinate of the apparent contact point $\mathbf{P}(X_{\text{f}}, Y_{\text{f}})$ on the constraint axis of the follower, where

$$Y'_{\text{f}} = Y_{\text{f}} + R_{\text{follower}} \sin\alpha = 61.0 \text{ mm} \tag{3}$$

$$X'_{\text{f}} = \frac{Y_{\text{f}} \sin\alpha + R_{\text{lever}} + R_{\text{follower}} \sin^2\alpha}{\cos\alpha} = 12.5 \text{ mm} \tag{4}$$

$$L_{\text{OP}'} = \sqrt{{X'_f}^2 + {Y'_f}^2} = 62.3 \text{ mm} \tag{5}$$

$$\beta = \tan^{-1} \frac{X'_{\text{f}}}{Y'_f} = 11.5^\circ \tag{6}$$

The actual moment arm L_{OQ} of T_{out} with elevation angle γ are also calculated by geometric relationships as follows:

$$\gamma = \tan^{-1} \frac{L_{\text{lever}} \sin\alpha}{Y_{\text{max}} - \delta} = 7.0^\circ \tag{7}$$

$$L_{\text{OQ}} = \frac{L_{\text{lever}} \sin\alpha}{\sin\gamma} = 95.0 \text{ mm} \tag{8}$$

By balancing the torques $T_{\text{in}} = T_{\text{out}}$ along **O**, the force applied on **Q** perpendicular to the moment arm is derived as $F_{\text{out}} = T_{\text{in}}/L_{\text{OQ}}$, and its effective component parallel to the translational direction of the finger as follows:

$$F'_{\text{out}} = F_{\text{out}} \cos\gamma = \frac{L_{OP'}}{L_{OQ}} F'_{\text{in}} \cos\gamma \tag{9}$$

Substituting the equations (2) and (6) in (1) yields $F'_{\text{in}} = 0.98\ F_{\text{in}}$, and then (1), (5), (7), and (8) in (9) gives $F'_{\text{out}} = 0.64 F_{in}$. This result indicates that the theoretical maximum transmission efficiency is 0.64, while the prototype model satisfies only 45.4% of this value with the basic structure but achieves 73.5% with the friction-improved version. In reality, the friction resistance proportional to the normal force $F_{\text{out}} \sin\gamma$, the counterforce of the ineffective component of F_{out}, should have decayed the clamping force by less than 1/8 of F'_{out}. Furthermore, mechanism deformations, such as bending of the lever and widening of the distance between the finger and the lever axis, result in the gradual decrease of the contact angle and thereby the inclination of the lever, as the F_{in} increases during clamping.

B. Disturbance on Compensation

The increase in power consumption from screw clamping was minimal because the spring cancelled out the additional load on the actuator caused by the magnet. The point to be considered is that the input force on the lever follower must have been approximately 150 N to exert the recorded output clamping force of 50 N on an average, according to Fig. 17, while the displacement-force characteristic of the pair of sampled magnets to which the spring was customized to follow, demonstrated a maximum value of 300 N.

The factors that may have affected the decrease in the input force are listed as follows. First, although mass-produced, the attraction force of magnets is known empirically to vary 250-300 N by individual difference. Second, the characteristic of each hand-made spring is designed to be less than the magnetic force for any displacement with feasible production conditions of error within 10%. Furthermore, the mechanism deformation leads to a subduction of the contact position X_{f} of the follower to the lever, which also results in the compressed length of the spring being less than designed.

Overall, preparing a more precise one-to-one spring specifically corresponding to the pair of magnets actually implemented in each gripper and reinforcing its mechanical rigidity yielded more energy-efficient and highly amplified clamping performance.

C. Selection of Actuators

For prototyping, a simple bidirectional screw driven by a DC motor was selected as an actuator, as it provides both sufficient torque and detailed positioning to conduct evaluation experiments. However, the way the IB magnet is used in the proposed gripper is categorized as a reduction mechanism, which does not restrict the actuator; any other actuator with even weaker output, such as artificial muscles made of shape-memory alloys, can be selected if the compensation spring is designed with higher precision. Moreover, if the clamping state has to be only on and off, two-state actuators without positioning ability, such as solenoids and pneumatics, can be selected. Furthermore, as the IB magnet can be activated even without electricity, the gripper can be powered by human power as a tool or by an external mechanical force as a passive mechanism.

D. Technological Value of the Outcome

In conjunction with the jumping mechanism [19] and the MR fluid gripper [20] proposed in our previous studies that incorporate the IB magnet as their magnetic flux supplier, the gripper in this study possesses a technological novelty in the idea of embedding the IB magnet as a built-in force amplifier, contrary to conventional applications of the IB magnets limited to attraction mechanisms. The amplifier can be easily implemented by including both the IB magnet and its attraction target inside the mechanism structure. Adjusting its magnitude of attraction by shifting the equilibrium point of compensation, the control rod, indirectly regulates the output force.

For the gripper, the difficulty of extracting a pressing force instead of non-contact magnetic force is that the output destination to be utilized is not the magnet but the fixed end of the spring, which is the outer frame of the IB magnet. As it is "fixed," its position has to be maintained at a certain position in the mechanism to establish a precise compensation, or its misalignment leads to the unsteady nonlinear output force with insufficient compensation, as observed in the previous design in Fig. 4(b). The desired application of the magnetic compensation mechanism as a gripper was finally achieved in this study by implementing the adjustment mechanism that made the position of the fixed end independent of the finger and the actual output destination.

These unprecedented applications of the IB magnet other than as attraction devices will contribute to the development of a new academic area of magnetic mechanisms, in which permanent magnets are used for reinforcement and energy conservation of robotic components that require large forces.

VI. Conclusion

For realizing energy-efficient robotic components that can be driven by a small, lightweight, and weak actuator, we have proposed the concept of a robotic gripper whose clamping operation is assisted by the attraction of a pair of permanent magnets, while their distance can be controlled by a minimal additional external force owing to internal balancing by a compensation spring. To achieve a more steady and predictable clamping force independent of the target object width, this study featured a new width adjustment mechanism using a lever toggle, which allows a mechanical separation of the fixed end of the compensation that generates the pressing force and the finger that actually exerts it on the object.

Experiments using the embodied prototype model were conducted to verify the amplification feature of its magnets on the clamping force and the compensation feature of its spring on the input control force. In particular, the gripper demonstrated that the magnetic assistance increased the maximum clamping force by 37.5%, while the spring compensation prevented the energy consumed by the actuator from increasing, resulting in the force-energy efficiency ratio multiplied by 1.39 in average, compared to the constitution without magnets. Furthermore, the width adjustment mechanism realized a linear width-force characteristic with a weak enough inclination and its lever-follower locking system exhibited a stable transmission efficiency, drastically making the clamping force more predictable and controllable than the gripper with the previous design.

In this manner, the proposed principle of the gripper was successfully validated, implying that replacing conventional grippers with the proposed system can contribute to a significant extension of the operation time of robots with limited power supply and a reduction in the electricity costs of robotic arms in production lines.

In future studies, we intend to adopt more accurate compensation, enhanced friction, and rigid structure to achieve even higher amplification rate and transmission efficiency using the discussed methods. A design with a more practical size and mass will be investigated for integration in robotic systems. In addition, a numerical model for estimating the exerted clamping force according to the elasticity of the mechanism and clamped object will be established to develop a control law. The applications of force amplification mechanisms will be further expanded to the studies of other energy-efficient robotic components and labor-saving tools.

References

[1] T. Takaki and T. Omata, "Linear motion mechanism with grasp force magnification," *J. Robot. Soc. Jpn.*, vol. 25, no. 2, pp. 299–305, 2007.

[2] T. Takayama, S. Makita, and T. Omata, "Development of a parallel jaw gripper with bidirectional force magnification mechanism," *Trans. Jpn. Soc. Mech. Eng. Ser. C*, vol. 76, no. 772, pp. 3542–3548, 2010.

[3] T. Takaki, T. Yamasaki, and I. Ishii, "Development of load-sensitive continuously variable transmission with oblique feed screw," in *Proc. JSME Annu. Conf. Robot. Mechatron.*, 2011, pp. 1A1–J04.

[4] T. Shimizu, K. Tadakuma, M. Watanabe, E. Takane, M. Konyo, and S. Tadokoro, "Internally-balanced magnetic mechanisms using a magnetic spring for producing a large amplified clamping force," in *Proc. IEEE Int. Conf. Robot. Automat.*, 2020, pp. 1840–1846.

[5] T. Shimizu, K. Tadakuma, M. Watanabe, E. Takane, M. Konyo, and S. Tadokoro, "Amplification of clamping mechanism using internally-balanced magnetic unit," in *Proc. IEEE Int. Conf. Intell. Robot. Syst.*, 2021, pp. 2765–2771.

[6] V. Arakelian, M. Dahan, and M. Smith, "A historical review of the evolution of the theory on balancing of mechanisms," in *Proc. Int. Symp. Hist. Mach. Mechanisms*, 2000, pp. 291–300.

[7] T. Aibara et al., "Development of a portable field arm with gravity compensation," in *Proc. JSME Annu. Conf. Robot. Mechatron.*, 2008, pp. 1A1–H01.

[8] S. Hirose, M. Imazato, Y. Kudo, and Y. Umetani, "Internally balanced magnetic unit," *J. Robot. Soc. Jpn.*, vol. 3, no. 1, pp. 10–19, 1985.

[9] K. Tadakuma and T. Tanaka, "IBM wheel : Mechanism of internal balanced magnetic wheel : Basic concept and the first prototype model," in *Proc. JSME Annu. Conf. Robot. Mechatron.*, 2014, pp. 1P2–O01.

[10] M. Ozawa, K. Tadakuma, Y. Okada, and S. Tadokoro, "Internally balanced magnetic crawler," in *Proc. IEEE 19th Annu. Conf. Sys. Integr. Division Soc. Instrum. Control Eng.*, 2017, pp. 1D5–108.

[11] K. Yanagimura, K. Ohno, Y. Okada, E. Takeuchi, and S. Tadokoro, "Hovering of MAV by using magnetic adhesion and winch mechanisms," in *Proc. IEEE Int. Conf. Robot. Automat.*, 2014, pp. 6250–6257.

[12] S. Murata, E. Yoshida, A. Kamimura, H. Kurokawa, K. Tomita, and S. Kokaji, "M-TRAN: Self-reconfigurable modular robotic system," *IEEE/ASME Trans. Mechatron.*, vol. 7, no. 4, pp. 431–441, Dec. 2002.

[13] T. Shimizu, K. Tadakuma, M. Watanabe, K. Abe, M. Konyo, and S. Tadokoro, "Permanent-magnetically amplified brake mechanism compensated and stroke-shortened by a multistage nonlinear spring," *IEEE Robot. Autom. Lett.*, vol. 7, no. 3, pp. 6266–6273, Jul. 2022.

[14] H. Arakawa, "One-way chuck," JP Patent S58-051470, Nov. 24, 1983.

[15] K. Yamamoto, "Linear clutch," JP Patent 2006132712A, May 25, 2006.

[16] I. Onda et al., "Force diode mechanism," in *Proc. JSME Annu. Conf. Robot. Mechatron.*, 2021, pp. 2P1–F06.

[17] K. Ito, "Linear clutch," JP Patent 2895509B2, May 24, 1999.

[18] M. Kawai, "The basic principle and example of torque diodes," in *Proc. JSME Ref. Collect. Annu. Meeting*, 2006, pp. 186–187.

[19] T. Shimizu et al., "Small swarm search robot system with rigid-bone parachute rapidly deployable from aerial vehicles," in *Proc. IEEE Int. Symp. Saf., Secur., Rescue Robot.*, 2019, pp. 88–93.

[20] T. Shimizu et al., "MR fluid jamming gripper applying internally-balanced magnetic unit controllable by small control force," in *Proc. JSME Annu. Conf. Robot. Mechatron.*, 2019, pp. 2A2–G03.